COBEM 2023 27TH INTERNATIONAL CONGRESS OF MECHANICAL ENGENEERING

ABCM Brazilian Society of Mechanical Sciences and Engineering
27th ABCM International Congress of Mechanical Engineering
December 04-08, 2023, Florianópolis-SC, Brazil

COB-2023-1121
NUMERICAL MODELING OF A LITHIUM-ION CELL USING AXIAL DIRECT COOLING STRATEGIES

Rodrigo Alonso Pires Júnior
Graduate Program of Mechanical Engineering at Universidade Federal de Minas Gerais
rodrigoalonsopires@ufmg.br

Braz de Jesus Cardoso Filho
Department of Electrical Engineering at Universidade Federal de Minas Gerais
braz.cardoso@ieee.org

Rudolf Huebner
Department of Mechanical Engineering at Universidade Federal de Minas Gerais
rudolf@demec.ufmg.br

Thales Alexandre Carvalho Maia
Department of Electrical Engineering at Universidade Federal de Minas Gerais
thalesmaiaufmg@gmail.com

Abstract. *Electrified vehicles tend to become the major land transportation way due to less environmental impact and higher operational efficiency. Lithium-ion batteries are one of the most common energy storage devices developed for these types of vehicles. In order to maximize battery storage lifetime and prevent premature failures, research efforts have focused on the degenerative phenomena characterization and ways to reduce these negative effects during operation. Most of these studies relate battery cell's temperature as one of the most important parameters associated with degradation phenomena, consequently, in the determination of battery's lifespan. Several experimental results presented in literature points that cooling strategies, in which the cells exchange heat directly with the fluid have greater efficiency and provide better temperature distribution over the pack. In order to propose a faster way to design a battery direct cooling system, this study presents a numerical cell's thermal model for axially direct cooling applications. To validate the presented model, experiments with a cell under forced convection are conducted using air as working fluid. A maximum error of 0.43 K in the cell's surface middle point temperature is encountered between the presented model and the measured on experimental tests.*

Keywords: *Electric vehicle, lithium-ion battery, heat generation, direct cooling, thermal modeling.*

1. INTRODUCTION

Global warming and air pollution is a high concern worldwide. According to IEA (2020) fossil fuel powered engines destined for transportation produce about 25% of total CO_2 global emissions. Between all transportation ways, land transportation including heavy and light vehicles represents 70% of total energy demand (Leach et al., 2020). In order to reduce GHG (Greenhouse Gas) emissions, new transportation strategies have been developed and vehicle electrification have been gaining prominence due to high energy efficiency, less environmental impact and lower mileage costs (Raugei et al., 2021). According to Wu et al. (2015) the electrification of a vehicle can be partial, known as hybrid vehicles, and total, known as electric vehicles. Studies presented in Ai et al. (2019) estimates that electrified vehicles will occupy about half of California's vehicle sales in 2040.

The fact that electrified vehicles are becoming attractive and market competitive is due to the use of Lithium-ion Batteries (LiBs) as internal storage devices (Muratori et al., 2020). Vehicle battery`s parameters like energy density, safety and lifespan had huge improvements with the use of Li-ion cells (Zhang et al., 2022). LiB`s cells are made by an anode, a cathode and a separator that works with the ion movement of cathode to anode while in charging operation or the other way around on discharging (Camargos et al., 2022). According to Liu et al. (2018) the lithium ion movement during operation produces heat that, if not controlled, can cause permanent damage to the storage device and lead to a safety issue known as Thermal Runaway.

In order to establish a solid way to determine the amount of heat produced by a LiB cell during operation, studies have been conducted throughout the years. A common way of heat generation estimation is to assume an internal resistance connected in series with the battery, in which all heat produced by the cell is due to this resistance, as seen in Noelle et al. (2018). As stated in Joule's Law, for a constant discharge rate the amount of heat produced is directly

proportional to the resistance. Aiming determines the internal resistance, studies conducted in Tafal (2019) noticed that the internal resistance has high correlation to the cell's State of Charge (SoC) and, mostly, with surface temperature. Given the high correlation to the cell's surface temperature, it can be assumed that the amount of heat generation can also be controlled by the battery cooling system.

Besides the heat generation, Waldmann et al. (2014) concluded that a cell's surface temperature is also directly linked to degradation. Cell's degradation can be understood as the loss of power storage capacity, also known as capacity loss. Regulations state that when a battery has a power storage capacity inferior to 80% relative to a brand new battery, that battery reaches its end of life and must be replaced. Through the work presented by Yin and Choe (2020), in which the author cycled a Li-ion cell over different temperature and discharge rate conditions. It can be observed that for each constant discharge rate point, degradation tends to rise similar to a second order function of temperature, as presented in Figure 1. This behavior indicates that there is an ideal temperature for each discharge rate, which the degradation is minimum. Is worth noting that the variable C stands for discharge rate, being the number before a multiplier given that 1C is the cell's nominal discharge rate in Ah.

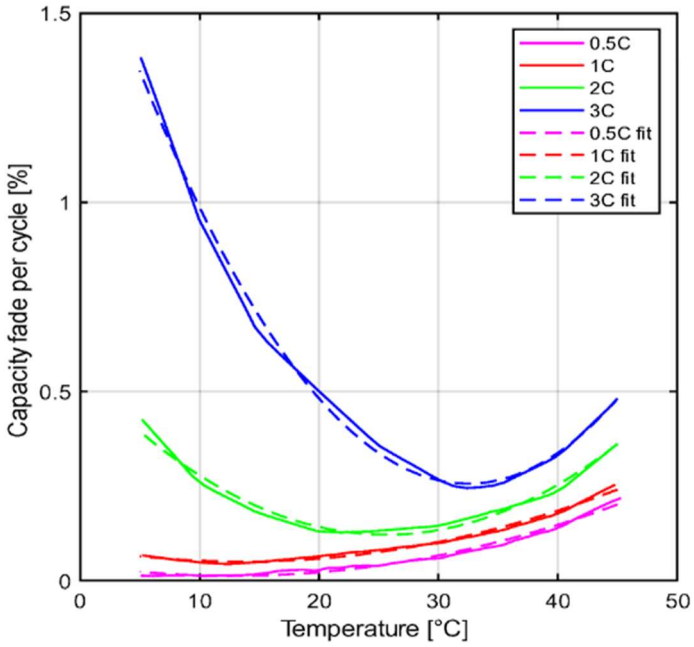

Figure 1. Degradation as a function of temperature over different discharge rates with second order polynomial fitting (Yin and Choe, 2020).

Given the importance of cell surface temperature control to extend battery`s lifetime and safety, cooling strategies have been developed. These strategies have the same structure in common, that is based on a circuit of a fluid in which it absorbs heat from the cells and rejects it to a colder source, in which could be the environment or another fluid. In terms of heat flow from cell to fluid, all strategies can be divided into two groups, the indirect and direct cooling strategies. As seen in the most common cooling solutions shown in Roe et al. (2019), in an indirect cooling system, the fluid doesn't have direct contact to the cells, and in a direct cooling strategy, there is direct contact between both interfaces. Even though direct cooling systems need to operate with dielectric fluids, results presented in Li et al. (2021) indicated that direct cooling strategies achieved better performance results than the indirect cooling ones.

Direct cooling systems for cylindrical cell type batteries can be designed in two different ways, in which the fluid flows in the cell`s radial direction or axial direction (Xia et al., 2017). Islava (2021) highlights that radial direct cooling systems have better surface temperature distribution than the axial direction systems due to the flow encountering more surface area at first. Although, radial direction flow systems have higher temperature differences between the first and last cell. Knowing that degradation phenomena rises when the cell's surface temperature is off the ideal temperature and usually vehicular battery cells cannot be replaced individually, a high temperature difference between cells can shorten the pack`s lifetime.

Even though the direct cooling systems have advantageous characteristics, there is still insufficient material related to this type of strategy in literature. Most studies related to it focus on experimental tests over specific conditions, as examples of works presented in Li et al. (2022). Although the experimental tests are crucial to the strategy validation, it cannot be used for different conditions, which precludes broader performance analysis.

In order to provide a performance calculation method suitable for any condition, the present work develops an axially direct cooling strategy model with the use of a numerical method based on CFD open source software OpenFOAM. The

numerical model bases on a cylindrical cell Panasonic NCR18650B and seeks to analyze the surface temperature profile as the internal temperature profile. Aiming the model`s validation, experimental tests are conducted using air as working fluid.

2. METHODOLOGY

2.1 Cylindrical cell`s thermophysical properties

Mekonnen et al. (2016) describes the build of a cylindrical lithium ion cell as a flat rectangle with three layers of materials, corresponding to the anode, separator and cathode, rolled over itself. This type of construction leads to difficulties in the thermophysical properties determination. As a way around to this issue, many authors developed experimental tests that aim to extract these parameters, as seen in Maleki et al. (1999). The experimental tests generate mean thermophysical values, which means that local values tend to be different to the extracted ones.

For specific heat capacity determination, many authors set tests that are based on the transient energy conservation equation. Maleki et al. (2019) related the cell heat loss by convection during the cooldown phase with the cell`s temperature drop rate, taking the parameter value out with the use of the energy balance equation. Drake et al. (2014) determined the specific heat capacity parameter in a similar way, but in this case the author uses the energy balance equation with the amount of energy used to heat the cell, instead of cooling it down.

Another crucial parameter related to the device`s thermal characteristics is the thermal conductivity. Given the construction characteristics, lithium ion cells are considered anisotropic devices, which means that the cells have different thermal conductivities in different directions. In the case of a cylindrical cell, since the construction is based on circular layers of different materials, the thermal conductivity is considered an orthotropic anisotropy in which this parameter varies only in the radial and axial directions. According to results shown in Spinner et al. (2016), the thermal conductivity in radial direction can be 10 to 50 times lower in relation to the axial direction thermal conductivity.

The thermal conductivity determination method is similar to the specific heat capacity test. According to Aiello et al. (2020), the method consists of the parameter estimation through the steady state energy balance equation. One thermal conductivity determination direction is chosen and the others are insulated, in order to minimize heat gradients in other directions. In order to determine the radial thermal conductivity, Murashko et al. (2020) involved the cell with a metallic shell and heated the outside temperature and measured the temperature in the contact interface between materials. Aiello et al. (2020) developed a similar experiment in which a heat flux sensor is placed on cell's both sides of the cell's aimed direction, and through the measured heat flux and temperatures, the parameters are taken through the steady-state energy conservation equation, which is simplified to the Fourier equation, as presented in the equation.

The present work will model a axially direct cooling strategy for cylindrical cells with experimental validation with the use of a commercial Li-ion cell. The cell used on tests is a Panasonic NCR18650B with nominal voltage of 3.7V and 3.2Ah capacity. In order to establish an accurate model and reduce the errors sources and magnitude, the model is based on thermal parameters extracted with experimental tests available in literature, as presented in Table 1.

Table 1. Thermo physical parameters considered based on Spinner et al. (2016).

Thermophysical properties	Value
Axial thermal conductivity, W/mK	5.1 ± 0.6
Radial thermal conductivity, W/mK	between 0.120 to 0.197
Specific heat capacity, K/kgK	727 ± 18
Specific mass, kg/m3	1593 ± 30

2.2 Cell heat generation modeling

Given the rise of performance of vehicular LiBs cooling strategies were developed to control the cell's heat generation. To reach the ideal cooling system performance parameters, it's ideal to determine the cell's amount of heat generation. In order to estimate it, Yang et al. (2019) considers the energy loss that is converted into heat as an internal resistance, given the high correlation to the cell's discharge current. According to Xie et al. (2018), the heat generation (Q_{cell}) is calculated by the sum of two factors, the first and more prominent, the Joule heating effect and the entropy generation rate during discharge, as presented in Eq. (1).

$$Q_{cell} = RI^2 + IT\frac{dU}{dt}. \tag{1}$$

The entropy generation rate can be described as a function of SoC, and its part in the energy equation can be neglected due to its magnitude (Redondo-Iglesias et al., 2020). Xie et al. (2018) determines the internal resistance by the potential difference between the cell's voltage in open circuit (OCV) and the voltage on discharge (V_t) divided by the instant

discharge, as presented in Eq. (2). The operational voltage (Vt) is not constant for all conditions and has high correlation to SoC and temperature (Taffal, 2019).

$$R = \frac{OCV - V_t}{I}. \tag{2}$$

In the case of the cell Panasonic NCR18650B, the parameter V_t value is presented in its datasheet, which makes possible the construction of internal resistance curves as function of SoC and temperature. Figure 2 presents the internal resistance value as a function of SoC and temperature obtained for the Panasonic NCR1865B cell presented in Pires Jr. et al. (2023).

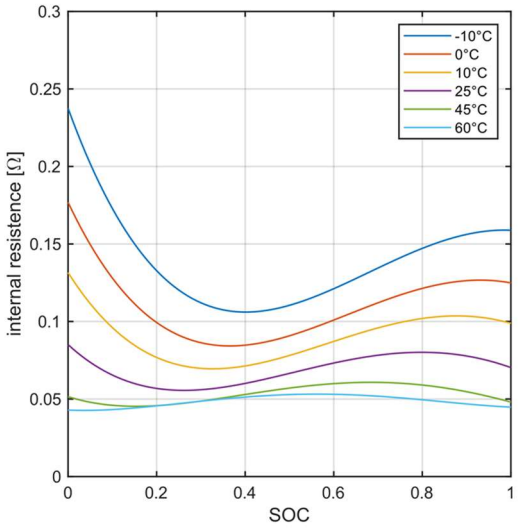

Figure 2. Panasonic cell internal resistance modeled in Pires Jr. et al. (2023).

2.3 **Problem definition**

The model's accuracy performance depends directly on the correct problem definition. Cooling systems are multi parameter architectures in which can be analyzed as a whole or interface individually. The present paper research interest focuses on the analysis of the heat exchange interface between cell and environment, which is a part of the entire battery cooling system, as presented in Figure 3. In order to justify the analysis and model development, the inlet parameters must be physically feasible to the entire cooling system, according to the output parameters obtained.

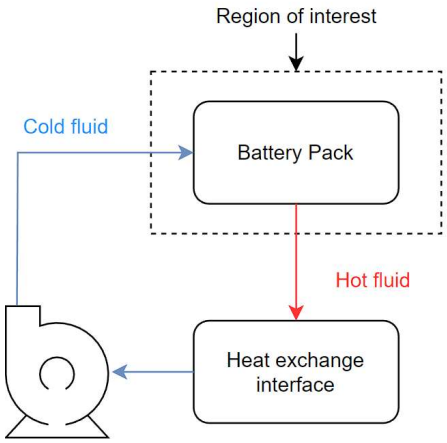

Figure 3. Battery cooling system analysis region of interest.

Even though numerical methods allow more flexibility in comparison to experimental methods, there are still costs and time involved. In that way, model simplifications can be used to reduce computational efforts and still obtain reliable results. In case of a LiB direct cooling system with axial flow direction, the analysis can be made for a single cell and

replicated to the others, as presented in Figure 4. This simplification is possible by the assumption of equally spaced cells, constant and uniform fluid's temperature and velocity at the inlet.

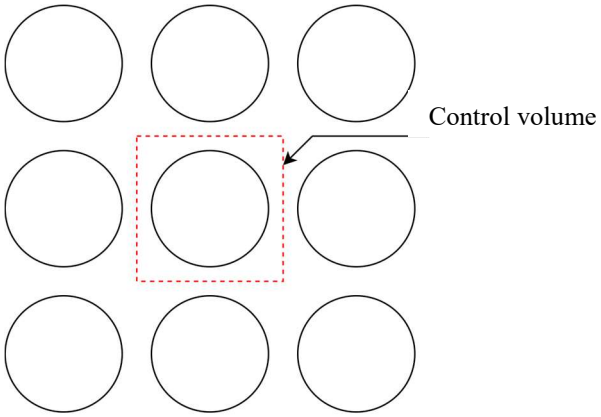

Figure 4. Problem`s control volume definition

Another model simplification made is that the heat exchange analysis occurs on steady state regime. Besides the computational saving, the steady state regime allows the determination of the expected temperature distribution inside the cell and on its surface. Another interesting parameter that the computational method obtains is the flow pattern and turbulence estimations.

2.4 **Computational method**

Computational methods are a proven tool to handle heat and mass transfer and fluid mechanics issues with high accuracy (Moukalled et al., 2016). These methods are suitable to estimate critical regions locations as well its magnitude over the rest of control volume, leading to quicker solutions development. Between all popular and used CFD softwares, OpenFOAM stands out as one of the most reliable open source softwares. In terms of conjugate heat transfer problems between solid and fluid, several studies available in literature attest the use of OpenFOAM as a reliable tool for this type of issues, as studies presented in Vendra et al. (2022).

Since the problem consists of the analysis of a cell under a forced convection flow, the control volume bases in a tube that constrains the flow with a cell inside. The cell modeling method is based on literature works that built the cell as a solid structure filled with an orthotropic material with different radial and axial thermal conductivities. As presented in Figure 5, according to the model presented in Panchal et al. (2018), a smaller cylinder is modeled in the cell's core. In the present model, the smaller cylinder is used to provide the heat interface though its walls. Another model simplification made is the disregard of the outside plastic shell.

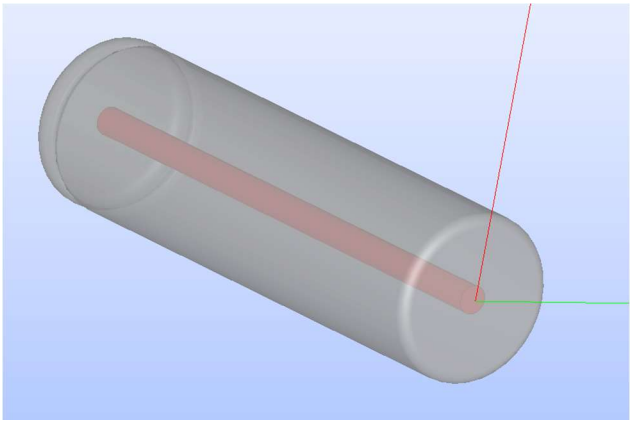

Figure 5. Computational cylindrical cell geometry developed.

The flow region construction is based on the 2 inch diameter pipe used in the experimental tests. At the inlet, constant value and uniform flow profile and temperature is setted as the boundary conditions. As presented in Figure 6, the cell and fluid region mesh max length is defined as equal to 0.05 times their respective diameter and a slow growth rate

between the cell and fluid is defined, in order to produce finer layers around the solid leading to a better results resolution output at the cell's surface.

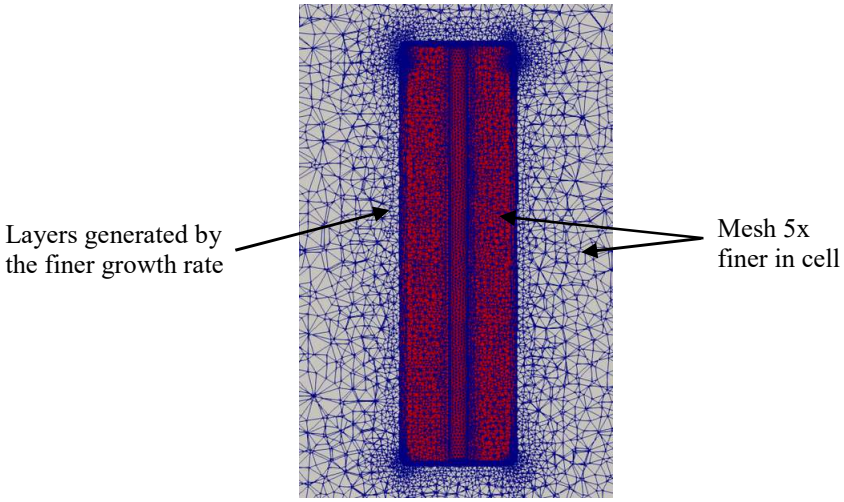

Figure 6. Cell mesh result.

Relating to the problem definition, the results are taken for a conjugated heat transfer between solid and fluid system in a steady state regime. The chosen solver is based on the SIMPLE algorithm and the turbulence k-ε equations, developed by Jones and Launder (1972), are used.

2.5 **Experimental setup**

In order to validate the presented model, an experimental setup is developed. The setup consists of a 2 inch diameter plastic pipe that houses the cell, being the pipe's inner bottom attached to a blower, as presented in Figure 7. A segment made of thinner tubes is placed after the blower aiming to provide an uniform velocity distribution in the bottom of the cell. The cell is positioned in the third pipe segment and, in order to minimize the flow perturbation by undesirable sources, the cell is kept suspended by only the electric connectors. In this way, magnetic connectors were developed to wire the cell to the discharging device as well as to maintain it at the pipe's center. The magnetic connectors also have the advantage of occupying a minor cell's surface area, having less interference at the heat exchange interface. The last pipe`s segment aims for the flow directioning and in the minimization of perturbations at the outlet.

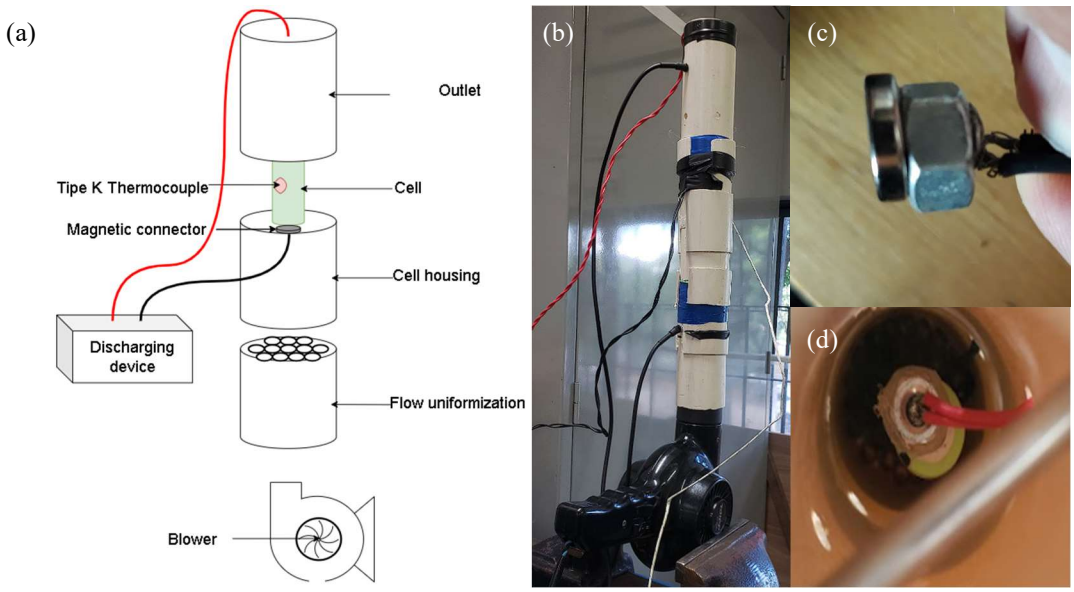

Figure 7. Experimental setup diagram (a), physical experimental setup (b), magnetic connect (c) and cell internal displacement (d).

The test rig aims to measure the cell's temperature rise when it reaches the steady-state regime. With that, a type K thermocouple is attached to the cell's surface middle point. The thermocouple data is interpreted by an Atmega32u4 with the use of a linear signal-conditioning interpreter module MAX6675, being the signal filtered via code. The initial thermocouple temperature is calibrated with the use of the thermometer MINIPA MT-401A. An anemometer, TESTO testo 416, is used to measure the flow velocity that will be fed in the CFD model inlet boundary conditions. The cell's surface temperature measurement uncertainty considered is 0.5 K, that is twice of the lowest equipment resolution value. The last equipment used is a cell capacity tester, model DL24P, that can supply constant current discharge at different discharge rates.

The experiment consists of the cell's surface temperature measurement while discharging until it reaches the steady-state regime. At the beginning of each experiment, the flow velocity is determined with the mean value of 8 different measurement points at the pipe`s outlet. Before the experiment starts, the blower is turned on while the capacity tester is off, aiming to ensure that the cell`s initial temperature is uniform and steady. In order to provide an adequate contact without temperature gradient generation, the contact between the thermocouple and the cell's surface is due to the constant applied force on the thermocouple terminal.

The experiments are taken with a Panasonic NCR18650B cell in which two discharge rates are tested, 1C and 1.5C. During all experiment duration, the input parameter data is collected within a 5 seconds interval. The experiment duration is determined when the temperature measurements reach its steady state or when the cell is completely discharged.

3. RESULTS AND DISCUSSION

From the experimental setup shown in topic 2.5, tests were taken for a constant 1C and 1.5C discharges that represents current magnitude of 3.2 A and 4.8 A respectively. The blower mean velocity taken at the outlet is 6 m/s. The ambient temperature is around 35 ºC and the internal resistance is considered constant with a value of 0.072 Ω. The temperature was collected at the cell`s middle surface point and its time evolution for each discharge is presented in Figure 8. In 1C test case, the cell's surface temperature reached a value of 307.45 K and in the case of 1.5C test, the temperature reached 312.06 K As expected, at higher discharge rates the cell's surface temperature elevation was higher, being at 1C discharge tests around 1.8 K and for the 1.5C discharge test, 5 K. It can be observed that the higher discharge rate test reached the steady-state regime twice as fast than the lower one. This fact can be related mainly to the sensor response at lower temperature delta between cell and environment. It is worth noting that the plots are similar to a first order transfer function, which can lead to the development of real time control applications. As observed at Figure 8(b), there is a temperature drop around 150 s that possibly relates to a loss of communication between the sensor and microcontroller. In that case, the signal does not fall directly to zero and instantaneously reaches the measure temperature due to the filter applied via code. Since the signal loss occurred within a small period, the overall result is not compromised.

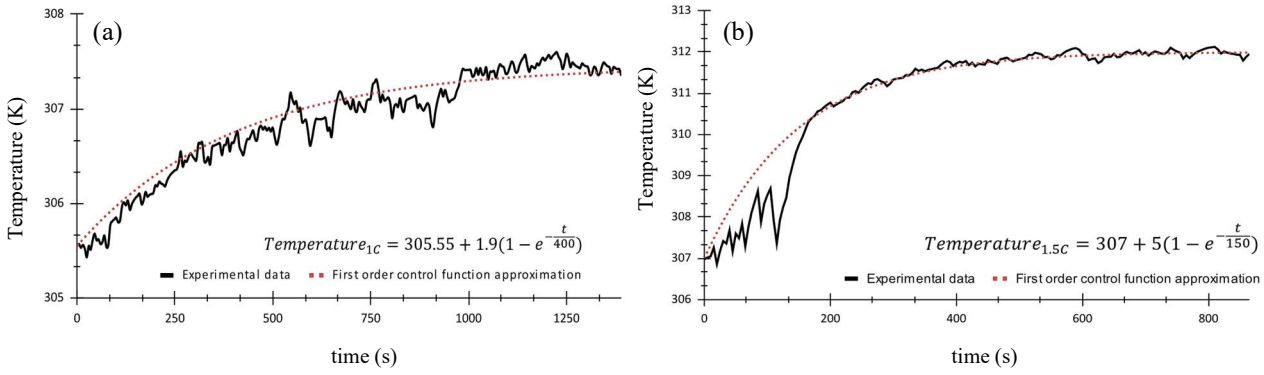

Figure 8. Experimental results for cell surface temperature evolution for 1C discharge rate (a) and 1.5C discharge rate (b).

With the key parameter taken for each experiment, the model verification started. The model's thermo physical variables were defined as the same values presented in Table 1, highlighting that the radial thermal conductivity value considered is 0.15 W/mK. The same experimental initial temperatures and flow velocities were taken in model`s inlet boundary conditions. According to the solver and simulations settings defined, Figure 9 (a) and (b) presents the cell's surface temperature in relation to its height (z positioned) and the cell's internal temperature at the middle height in relation to its radius for both, 1C and 1.5C, discharge rates. The results show that, at the middle surface point, for 1C discharge rate, the obtained temperature value is 307.88 K, 0.43 K difference from the experimental results. In case of 1.5C discharge rate regime, the temperature value reached is 312.28 K, 0.22 K off the experimental value obtained.

Through the internal temperature analysis, presented in Figure 9 (c) and (d), a higher temperature gradient is observed between core and surface for 1.5C discharge rate, as expected. For 1C discharge rate the temperature gradient reached 15

K in comparison to more than 30 K, observed for 1.5C discharge rate. Given the model heat generation assumption occurrence in the interface between core and cell, the temperature decreases with respect to the logarithm function. This characteristic is in accordance with Fourier's law, as presented in Kakaç and Yener (2018) for a one dimension cylinder with cladding case deduction.

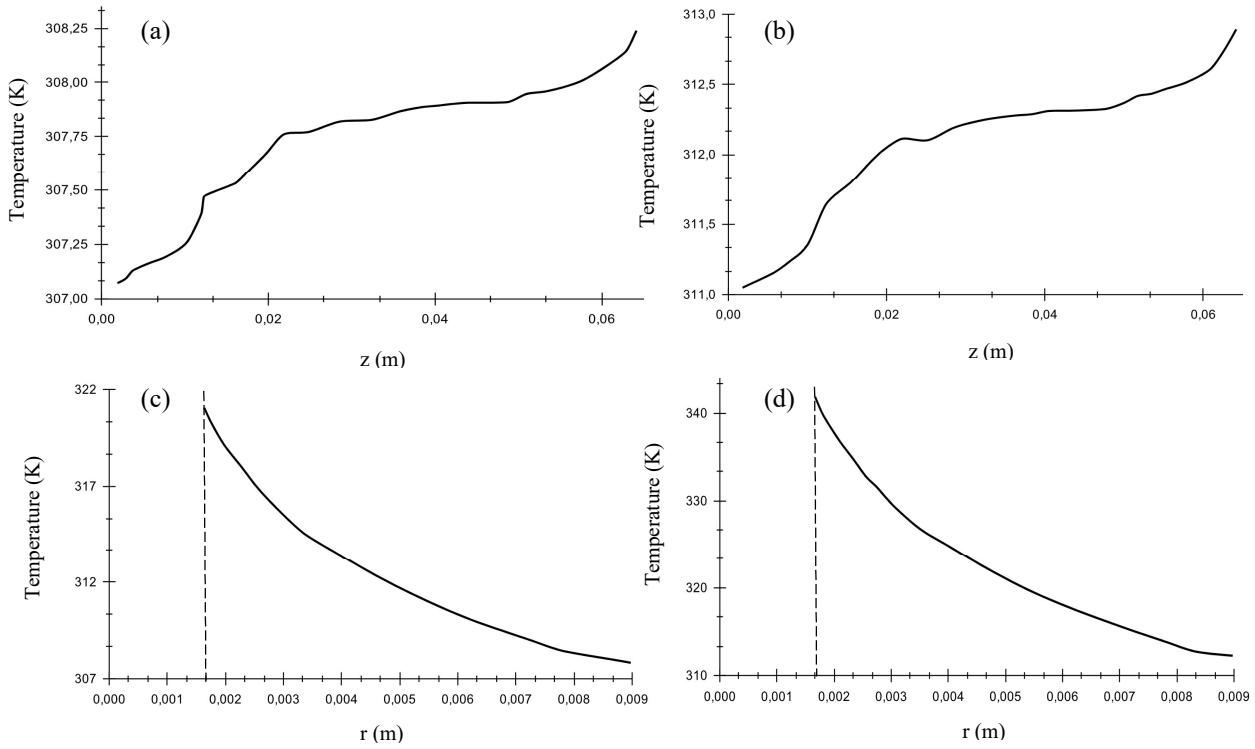

Figure 9. CFD's temperature distribution on the cell's surface for 1C discharge (a) and 1.5C discharge (b) and internal temperature distribution for 1C discharge (c) and 1.5C discharge (d).

Some hypotheses can be made through the results difference, being the first one the divergence in the real temperature point taken in the experiment and the point defined in the CFD model, which is more location precise and has no signal reading errors. As any thermocouple, the measured temperature is influenced by the device`s contact surface, in the experiment case, considering a sphere contact, the smaller part is in contact with the cell and the rest is in contact with the air flow. This assumption justifies the bigger disparity in the 1C discharge case, in which the temperature gradient between cell and air is smaller, in comparison to the 1.5C discharge rate test. Like every experiment, there are also error sources that can deviate the result, such as the contact between thermocouple and cell, the signal loss throughout the thermocouple wiring and connection and the error associated with the microprocessor value interpretation. In relation to numerical solutions, the discretization is an error source along with the model simplifications made. Another logical hypothesis that can be raised is the disparity between the model`s thermo physical parameters and internal resistance values and these cell`s actual values. It is worth noting that the result disparity can be a consequence of the combination of all hypotheses raised.

With the error deviation possible sources cited, it is possible to verify the model's reliability. The verification can be based on the error between the experiment and the CFD results. The maximum error seen in temperature difference between methodologies is 0.43 K for the 1C discharge rate. Given the fact that the usual measurement uncertainty of a type K thermocouple is around 1.5 K, the deviation between model and experiment is within the device's accuracy range.

Figure 10 presents the temperature distribution in a cross cut in isometric view of the cell for 1C and 1.5C discharge rate. In consonance with the previous figures, for 1C discharge rate, the surface temperature gradient is almost the half of the 1.5C discharge rate surface temperature gradient. Also, for the higher current rate case, the internal temperature close to the cell's core is 20 K higher than the other case.

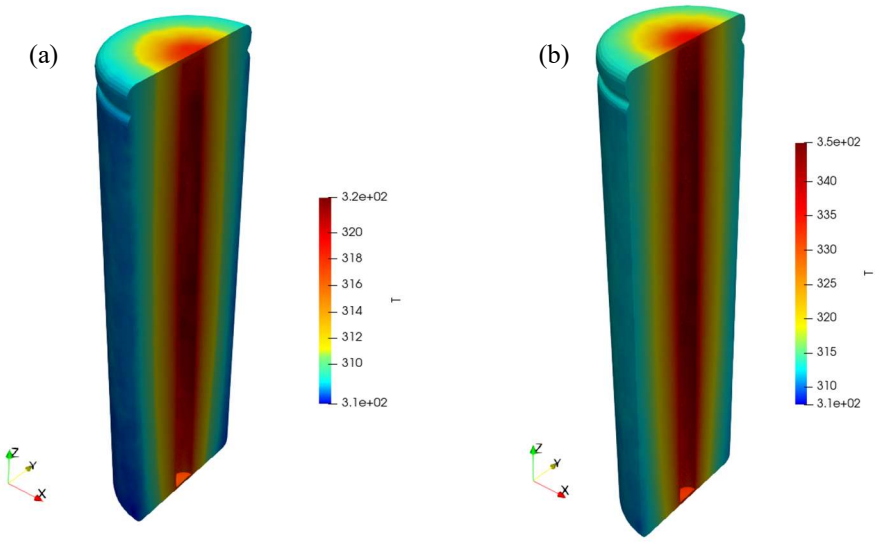

Figure 10. CFD results as graphical temperature distribution.

As the comparison of experimental and the CFD model results, the model's validity is attested for the experimental conditions proposed. With validation, the model can be used as a tool to broader analysis and the development of new related cooling strategies acceleration. As an example of the CFD model reliability, the performance comparison of different commercial dielectric cooling fluids under different discharge rate and environment conditions, can be done without the need of an experimental rig and with more parameters detailing, such as temperature and velocity, accelerating the development of new solutions.

4. CONCLUSION

Given the raise of environmental preservation awareness, electrified vehicles tend to become the major urban transportation way. The use of high performance LiBs on these types of vehicles raise concerns about the temperature maintenance of these devices. As direct cooling strategies are proven one of the most efficient ways to cool these storage devices, this paper presented a CFD cylindrical cell model construction methodology with experimental validation.

The tests are conducted with a Panasonic NCR18650B cell, in which the model's thermo physical parameters were taken in previous works available in literature. The current experiment done in this paper aimed to obtain the cell's surface middle temperature point gradient between the initial and steady-state conditions. In order to provide a solid validation analysis, tests are run for two different discharge regimes, 1C and 1.5C.

The results comparison between CFD and the experiments showed a maximum error of 0.43 K in the temperature measurement at the cell's middle surface point. This difference is lower than the thermocouple uncertainty measurement, which corroborates to the model's validity. The raised disparity occurrence hypothesis bases on the contact interface between the thermocouple and cell, as the experimental errors sources. Also, the difference between cell's actual thermal properties and the data taken from literature could be the cause of this issue.

With the model's validation, as an advantage of numerical models, several analyses linked to direct cooling strategies can be done. As a work continuation, new fluids under different environment and operational conditions can be tested as well as the verification of the system under dynamic response in transient regimes.

5. REFERENCES

AI, Ning; ZHENG, Junjun; CHEN, Wei-Qiang. US end-of-life electric vehicle batteries: Dynamic inventory modeling and spatial analysis for regional solutions. Resources, Conservation and Recycling, v. 145, p. 208-219, 2019.

AIELLO, Luigi et al. In situ measurement of orthotropic thermal conductivity on commercial pouch lithium-ion batteries with thermoelectric device. Batteries, v. 6, n. 1, p. 10, 2020.

CAMARGOS, Pedro H. et al. Perspectives on Li-ion battery categories for electric vehicle applications: A review of state of the art. International Journal of Energy Research, v. 46, n. 13, p. 19258-19268, 2022.

DRAKE, S. J. et al. Measurement of anisotropic thermophysical properties of cylindrical Li-ion cells. Journal of Power Sources, v. 252, p. 298-304, 2014.

IEA (2021) Greenhouse gas emissions from Energy Data Explorer – Data Tools, IEA. Available at: https://www.iea.org/data-and-statistics/data-tools/greenhouse-gas-emissions-from-energy-data-explorer (Accessed: 09 June 2023).

ISLAVA, Holden; ISLAVA, Holden Alphonse. Radial vs. axial cooling for 18650 lithium ion battery cells. 2021. Tese de Doutorado.

JONES, W. Peter; LAUNDER, Brian Edward. The prediction of laminarization with a two-equation model of turbulence. International journal of heat and mass transfer, v. 15, n. 2, p. 301-314, 1972.

KAKAÇ, Sadık; YENER, Yaman; NAVEIRA-COTTA, Carolina P. Heat conduction. CRC press, 2018.

LEACH, Felix et al. The scope for improving the efficiency and environmental impact of internal combustion engines. Transportation Engineering, v. 1, p. 100005, 2020.

LI, Yang et al. Three-Dimensional Thermal Simulations of 18650 Lithium-Ion Batteries Cooled by Different Schemes under High Rate Discharging and External Shorting Conditions. Energies, v. 14, n. 21, p. 6986, 2021.

LI, Yang et al. Experimental studies of liquid immersion cooling for 18650 lithium-ion battery under different discharging conditions. Case Studies in Thermal Engineering, v. 34, p. 102034, 2022.

LIU, Xiang et al. Thermal runaway of lithium-ion batteries without internal short circuit. Joule, v. 2, n. 10, p. 2047-2064, 2018.

MALEKI, Hossein et al. Thermal properties of lithium-ion battery and components. Journal of the Electrochemical Society, v. 146, n. 3, p. 947, 1999.

MEKONNEN, Yemeserach; SUNDARARAJAN, Aditya; SARWAT, Arif I. A review of cathode and anode materials for lithium-ion batteries. SoutheastCon 2016, p. 1-6, 2016.

MOUKALLED, Fadl et al. The finite volume method. Springer International Publishing, 2016.

MURASHKO, Kirill A.; PYRHÖNEN, Juha; JOKINIEMI, Jorma. Determination of the through-plane thermal conductivity and specific heat capacity of a Li-ion cylindrical cell. International Journal of Heat and Mass Transfer, v. 162, p. 120330, 2020.

MURATORI, Matteo et al. The rise of electric vehicles—2020 status and future expectations. Progress in Energy, v. 3, n. 2, p. 022002, 2021.

NOELLE, Daniel J. et al. Internal resistance and polarization dynamics of lithium-ion batteries upon internal shorting. Applied energy, v. 212, p. 796-808, 2018.

PANCHAL, S. et al. Electrochemical thermal modeling and experimental measurements of 18650 cylindrical lithium-ion battery during discharge cycle for an EV. Applied Thermal Engineering, v. 135, p. 123-132, 2018.

RAUGEI, Marco; KAMRAN, Mashael; HUTCHINSON, Allan. Environmental implications of the ongoing electrification of the UK light duty vehicle fleet. Resources, Conservation and Recycling, v. 174, p. 105818, 2021.

REDONDO-IGLESIAS, Eduardo; VENET, Pascal; PELISSIER, Serge. Modelling lithium-ion battery ageing in electric vehicle applications—calendar and cycling ageing combination effects. Batteries, v. 6, n. 1, p. 14, 2020.

ROE, Charlotte et al. Immersion cooling for lithium-ion batteries–A review. Journal of Power Sources, v. 525, p. 231094, 2022.

SPINNER, Neil S. et al. Novel 18650 lithium-ion battery surrogate cell design with anisotropic thermophysical properties for studying failure events. Journal of Power Sources, v. 312, p. 1-11, 2016.

TAFFAL, Mohammad. Electro-Thermal Modeling of Lithium-Ion Battery. 2019. Tese de Doutorado. Politecnico di Torino.

VENDRA, Chandra MR et al. Numerical and experimental characterisation of high energy density 21700 lithium-ion battery fires. Process Safety and Environmental Protection, v. 160, p. 153-165, 2022.

WALDMANN, Thomas et al. Temperature dependent ageing mechanisms in Lithium-ion batteries–A Post-Mortem study. Journal of power sources, v. 262, p. 129-135, 2014.

WU, Guang; ZHANG, Xing; DONG, Zuomin. Powertrain architectures of electrified vehicles: Review, classification and comparison. Journal of the Franklin Institute, v. 352, n. 2, p. 425-448, 2015.

XIA, Guodong; CAO, Lei; BI, Guanglong. A review on battery thermal management in electric vehicle application. Journal of power sources, v. 367, p. 90-105, 2017.

XIE, Yi et al. A novel resistance-based thermal model for lithium-ion batteries. International Journal of Energy Research, v. 42, n. 14, p. 4481-4498, 2018.

YANG, Naixing et al. An improved semi-empirical model for thermal analysis of lithium-ion batteries. Electrochimica Acta, v. 311, p. 8-20, 2019.

YIN, Yilin; CHOE, Song-Yul. Actively temperature controlled health-aware fast charging method for lithium-ion battery using nonlinear model predictive control. Applied energy, v. 271, p. 115232, 2020.

ZHANG, Xinghui et al. A review on thermal management of lithium-ion batteries for electric vehicles. Energy, v. 238, p. 121652, 2022.

6. RESPONSIBILITY NOTICE

The authors are the only responsible for the printed material included in this paper.